Nucleation in mesoscopic systems under transient conditions: Peptide-induced pore formation in vesicles

Vladimir P. Zhdanov[1,2,*] and Fredrik Höök[1,*]

[1]*Department of Applied Physics, Chalmers University of Technology, S-41296 Göteborg, Sweden*
[2]*Boreskov Institute of Catalysis, Russian Academy of Sciences, Novosibirsk 630090, Russia*

Attachment of lytic peptides to the lipid membrane of virions or bacteria is often accompanied by their aggregation and pore formation, resulting eventually in membrane rupture and pathogen neutralization. The membrane rupture may occur gradually via formation of many pores or abruptly after the formation of the first pore. In academic studies, this process is observed during interaction of peptides with lipid vesicles. We present an analytical model and the corresponding Monte Carlo simulations focused on the pore formation in such situations. Specifically, we calculate the time of the first nucleation-limited pore-formation event and show the distribution of this time in the regime when the fluctuations of the number of peptides attached to a vesicle are appreciable. The results obtained are used to clarify the mechanism of the pore formation and membrane destabilization observed recently during interaction of highly active α-helical peptide with sub-100-nm lipid vesicles that mimic enveloped viruses with nanoscale membrane curvature. The model proposed and the analysis presented are generic and may be applicable to other meso- and nanosystems.

PACS number(s): 87.14.Cc, 64.60.Q−, 87.14.ef

I. INTRODUCTION

Nucleation of a new phase, occurring under thermodynamically favorable conditions, is a basic physicochemical phenomenon. It is observed in very different systems and accordingly plays an important role in numerous applications. For these reasons, the studies of this process have a long history spanning over 280 years (reviewed in Ref. [1]). The classical nucleation theory (CNT) was developed over 80 years ago by Volmer, Weber, Becker, Doering, and Zeldovich (reviewed in Ref. [2]). At present, this area continues to attract attention in efforts to clarify the mechanistic details (in addition to reviews [1,2], see, e.g., the nucleation theorems discussed by Ford [3], more recent general studies [4], a review of the kinetics of protein aggregation [5], and references therein). The corresponding treatments usually imply that a medium is macroscopic, nucleation occurs under steady-state conditions, the subcritical nuclei of a new phase are at equilibrium with an original metastable phase, and the number of atoms or molecules in a critical nucleus is large. Under such conditions, the nucleation rate is expressed via the free energy of formation of the critical nuclei.

During the past decade, the focus of studies in natural sciences has appreciably shifted to physicochemical and biological meso- and nanosystems. In such systems, nucleation often also may play an important role (see, e.g., the analysis of melting and freezing of metal nanoparticles [6], protein folding [7], and lipid self-assembly [8]). The interpretation of the corresponding experimental results is often possible in the framework of the general CNT concepts (for the shortcoming of CNT, see, e.g., the review by Ford [2]). The practical realization of these concepts should, however, as a rule include novel ingredients taking the specifics of meso- or nanosystems into account.

To motivate our work, we refer to the experimental studies of interaction of lytic peptides with lipid vesicles, viral membranes, or bacteria (see reviews [9], recent experiments [10,11], related molecular dynamics simulations [12], and references therein). In these systems, the attachment of peptides to the membrane is accompanied by their aggregation, pore formation, and, sometimes, membrane rupture, which in the case of bacteria and virions leads to pathogen neutralization. The process may occur gradually via formation of many pores or abruptly via membrane rupture followed the formation and growth of the first pore. These two scenarios can experimentally be distinguished and tracked by using single-vesicle imaging as shown in recent experiments [11] with highly active α-helical peptide and sub-100-nm vesicles. Theoretically, the corresponding kinetics or at least the pore-formation events can be described in the terms of nucleation theory. Direct application of CNT may, however, be hampered here because (i) the nucleation resulting in pore formation occurs under transient peptide-attachment conditions, (ii) the number of peptides (per vesicle or virion) is relatively small (from a few hundred to a few thousand), (iii) there may be only a few precritical nuclei, and (iv) the critical nucleus may include only a few peptides. For the first scenario implying the vesicle rupture following the formation of many pores, reservations of this type are often not crucial (especially if one is primarily interested in rupture) and the corresponding models have already been proposed and correlated with experimental results (see, e.g., Ref. [13]). For the second scenario with the rupture following the formation of the first pore, the reservations indicated are more restrictive and, in addition, some of the questions raised are different from those customarily addressed by CNT. For example, the nucleation rate is not central in this case. What is often more interesting and practically important is the time of the first nucleation event, referred to below as the first-passage time $t_{\rm FP}$, and the distribution of this time related to fluctuations of the number of peptides associated with a vesicle.

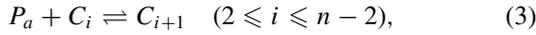*zhdanov@catalysis.ru; fredrik.hook@chalmers.se

Employing a generic kinetic model of peptide-induced and nucleation-limited pore formation in vesicles, we have recently derived an analytical expression for t_{FP} [11]. In our present work, using the same model, we briefly describe and extend the earlier analysis [Eqs. (1)–(11) in Sec. II], derive analytical expressions allowing one to estimate the role of fluctuations in the distribution of t_{FP} [Eqs. (12)–(14) in Sec. II], present Monte Carlo (MC) simulations (Sec. III) focused on these aspects of the kinetics, and illustrate how the results obtained may help to interpret the experiment (Sec. IV).

II. ANALYTICAL RESULTS

Let us consider attachment of peptides to a vesicle. This process is assumed to be irreversible and schematically represented as

$$P_s \rightarrow P_a, \tag{1}$$

where P_s and P_a are peptides in the solution and on the membrane. The pore formation is considered to be limited by nucleation including $n - 1$ sequential steps of association of P_a and i-mers,

$$P_a + P_a \rightleftharpoons C_2, \tag{2}$$

$$P_a + C_i \rightleftharpoons C_{i+1} \quad (2 \leqslant i \leqslant n - 2), \tag{3}$$

$$P_a + C_{n-1} \rightarrow C_n, \tag{4}$$

where C_i ($2 \leqslant i \leqslant n - 1$) is an i-mer containing i monomers. Step (4) is assumed to be slow compared to steps (2) and (3). After step (4), the pore-formation process may include association of additional peptides. The latter steps are considered to be rapid and not treated explicitly.

Initially (at $t = 0$), a vesicle is set to be free of peptides. The nucleation is assumed to occur when the number of peptides attached to a vesicle becomes appreciable, $N \gg n$ (note that a critical nucleus typically includes only a few peptides, i.e., n is usually smaller than 10, which makes $N \gg n$ a valid assumption even if N is relatively small). In analogy with CNT, we consider that the attached peptides are primarily monomers. In other words, this means that the peptide uptake is approximately equal to the number of monomers $N \simeq N_1$. With this condition, the peptide uptake [step (1)] is described phenomenologically as

$$N_1 = A t^\alpha, \tag{5}$$

where A is a constant and α is the corresponding exponent. For example, $\alpha = 1$ corresponds to the simplest kinetically limited attachment kinetics or the diffusion-limited kinetics under the flow conditions, while $\alpha = 1/2$ may describe the diffusion-limited case under no flow conditions.

In analogy with CNT, we consider that steps (2) and (3) are close to equilibrium. In this case, the number of C_{n-1} is given by

$$N_{n-1} = K N_1^{n-1}, \tag{6}$$

where K is the equilibrium constant for the formation of C_{n-1}. Substituting (5) into (6) yields

$$N_{n-1} = K A^{n-1} t^{\alpha(n-1)}. \tag{7}$$

The equation for the number of C_n is read as

$$dN_n/dt = k_n N_{n-1} N_1, \tag{8}$$

where k_n is the rate constant of step (4). Substituting (5) and (7) into (8) results in
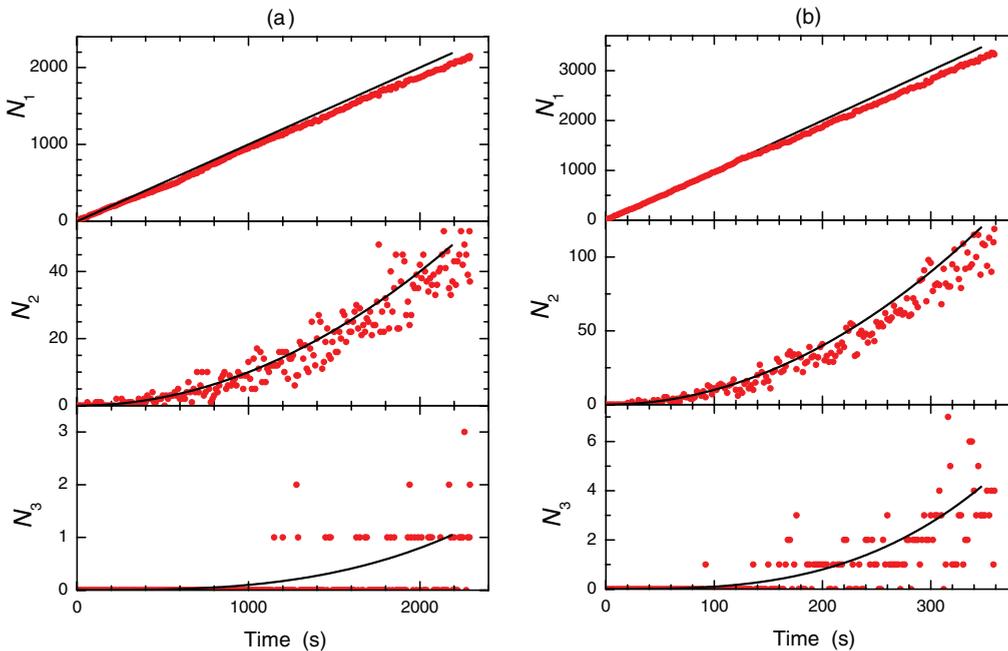
$$dN_n/dt = k_n K A^n t^{\alpha n}. \tag{9}$$

FIG. 1. (Color online) Typical dependences of N_1, N_2, and N_3 on time for $r_a = 1$ (a) and 10 s^{-1} (b). The MC kinetics (circles) were calculated up to the first pore-formation event. The interval between the MC data point is 10 s. The MF kinetics (lines) were calculated by using Eqs. (19)–(22) up to $N_4 = 1$.

Integrating (9), we obtain

$$N_n = k_n K A^n t^{\alpha n+1}/(\alpha n + 1). \tag{10}$$

The time of the first nucleation event or, in other words, the first-passage time can be identified with reaching $N_n = 1$. Using this condition and Eq. (10), we have

$$t_{FP} = \left(\frac{\alpha n + 1}{k_n K A^n} \right)^{1/(\alpha n+1)}. \tag{11}$$

In fact, this expression represents the average mean-field (MF) first-passage time.

In an ensemble of identical vesicles, t_{FP} is distributed due to fluctuations of the number of peptides attached to a vesicle. The important point is that the nucleation occurs primarily near the average first-passage time $\langle t_{FP} \rangle$ because the nucleation rate [Eq. (8)] becomes appreciable when $t \simeq \langle t_{FP} \rangle$. According to Eq. (8), the time scale of nucleation is equal to $1/(k_n N_{n-1} N_1)$. At $t \simeq \langle t_{FP} \rangle$, N_1 is much larger than N_{n-1} and, accordingly, the fluctuations of N_1 are negligible, i.e., one can replace N_1 by $\langle N_1 \rangle$. The fluctuations of $1/N_{n-1}$ can be estimated by expanding this ratio and taking into account the part related to fluctuations, i.e., $\Delta N_{n-1}/\langle N_{n-1} \rangle^2$. Following this line, we represent the deviation of t_{FP} as $\Delta t_{FP} = \Delta N_{n-1}/k_n \langle N_1 \rangle \langle N_{n-1} \rangle^2$. The standard deviation of t_{FP}

is accordingly given by

$$\langle (\Delta t_{FP})^2 \rangle^{1/2} = \frac{\langle (\Delta N_{n-1})^2 \rangle^{1/2}}{k_n \langle N_1 \rangle \langle N_{n-1} \rangle^2}. \tag{12}$$

Dividing the left and right parts of this expression by $\langle t_{FP} \rangle$ and using Eqs. (5), (7), and (11), one can rewrite it as

$$\frac{\langle (\Delta t_{FP})^2 \rangle^{1/2}}{\langle t_{FP} \rangle} = \frac{\langle (\Delta N_{n-1})^2 \rangle^{1/2}}{(\alpha n + 1)\langle N_{n-1} \rangle}. \tag{13}$$

The latter expression indicates that the normalized standard deviation of t_{FP} is smaller than that of N_{n-1} by a factor of $\alpha n + 1$.

The analysis above implies that the variance $\langle (\Delta N_{n-1})^2 \rangle$ should be calculated by employing the N_{n-1} values corresponding to the nucleation events. Thus the distribution of N_{n-1} is expected to be slightly different compared to the equilibrium distribution because the nucleation events are more probable for larger N_{n-1} and there may be deviations from equilibrium. This difference is, however, expected to be minor and $\langle (\Delta N_{n-1})^2 \rangle$ can be calculated by using the Poissonian distribution corresponding to equilibrium, i.e.,

$$\langle (\Delta N_{n-1})^2 \rangle = \langle N_{n-1} \rangle. \tag{14}$$

The formulas derived above allow one to calculate the average time of the first nucleation event, resulting in the pore formation, and its standard deviation. If the vesicle rupture
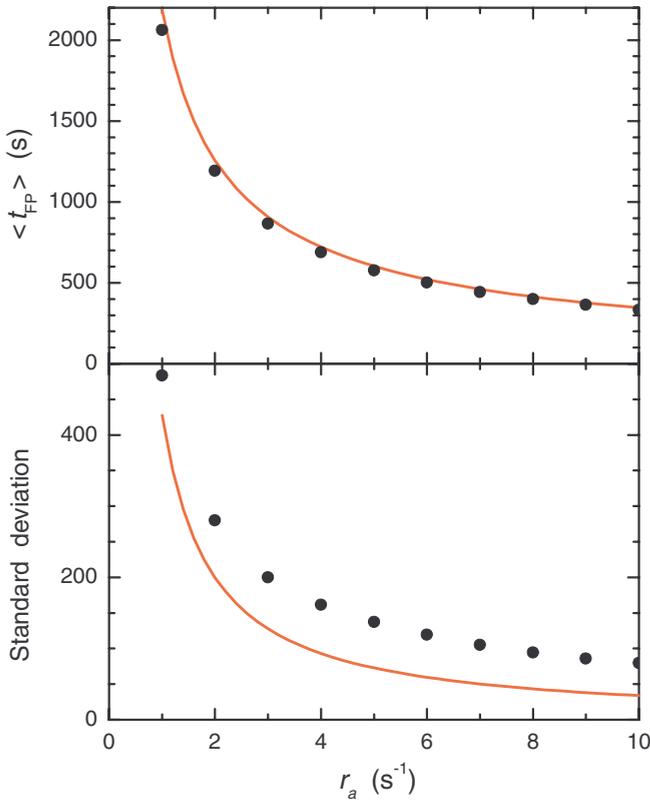

FIG. 2. (Color online) Average first-passage time and its standard deviation as a function of the attachment rate. The MC and MF data are shown by circles and lines, respectively. Each MC data point was obtained by using 5×10^3 MC runs. In the MF case, $\langle t_{FP} \rangle$ was calculated by using Eq. (23) and its standard deviation was obtained by employing Eqs. (12), (14), and (21).
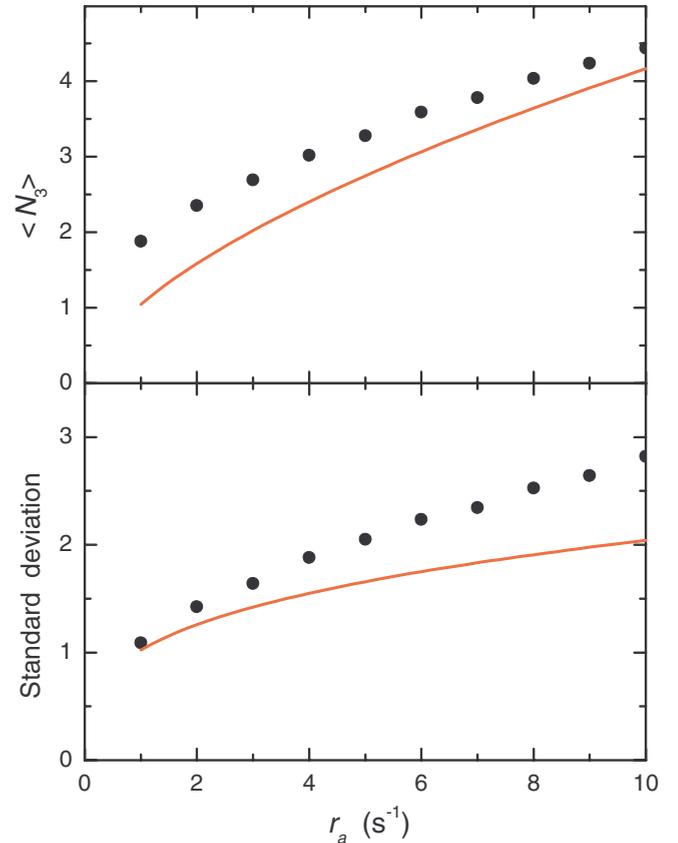

FIG. 3. (Color online) Average number of precritical nuclei and its standard deviation as a function of the attachment rate. Each MC data point was obtained by using 5×10^3 MC runs. The MF curves were constructed by employing Eqs. (21) and (14).

occurs just after the formation of the first pore, the formulas can also be directly used to interpret rupture.

III. MONTE CARLO SIMULATIONS

The accuracy of some of the steps in our analysis above can be debated. For example, the number of subcritical nuclei N_{n-1} during the nucleation event may be low (from one to a few copies) and one may doubt whether the MF equations are accurate in this limit. To scrutinize such aspects, we have performed MC simulations of the kinetics under consideration in the case when N_{n-1} is indeed low. The advantage of the MC technique is that it allows us to simulate steps (1)–(4) exactly without the simplifications inherent to the MF treatment.

For example, we analyze nucleation with $n = 4$ (this value of n was used to interpret the experiments in Ref. [11]). The peptide attachment to a vesicle is considered to be kinetically limited, i.e., $\alpha = 1$. The corresponding MF equations for the i-mer populations are

$$dN_1/dt = r_a - 2k_2 N_1^2 + 2d_2 N_2 - k_3 N_2 N_1$$
$$+ d_3 N_3 - k_4 N_3 N_1, \quad (15)$$

$$dN_2/dt = k_2 N_1^2 - d_2 N_2 - k_3 N_2 N_1 + d_3 N_3, \quad (16)$$

$$dN_3/dt = k_3 N_2 N_1 - d_3 N_3 - k_4 N_3 N_1, \quad (17)$$

$$dN_4/dt = k_4 N_3 N_1, \quad (18)$$

where r_a is the attachment rate and k_i and d_i are the peptide association and dissociation rate constants. Employing these

equations and following the prescriptions described in Sec. II, we have

$$N_1 = r_a t, \quad (19)$$

$$N_2 = k_2 (r_a t)^2 / d_2, \quad (20)$$

$$N_3 = k_2 k_3 (r_a t)^3 / d_2 d_3, \quad (21)$$

$$N_4 = k_2 k_3 k_4 r_a^4 t^5 / 5 d_2 d_3, \quad (22)$$

$$t_{\rm FP} = \left(\frac{5 d_2 d_3}{k_2 k_3 k_4 r_a^4} \right)^{1/5}, \quad (23)$$

where $r_a \equiv A$ and $K \equiv k_2 k_3 / d_2 d_3$.

Our MC simulations are based on the standard Gillespie algorithm including the calculation of the total rate of all the possible steps $w_t = \sum_i w_i$, realization of one of the steps chosen with probability w_i / w_t, and the increment of time by $|\ln(\rho)|/w_t$, where ρ ($0 < \rho \leqslant 1$) is a random number. In our case, we have six steps occurring with the rates $w_1 = r_a$, $w_2 = k_2 N_1 (N_1 - 1)$, $w_3 = d_2 N_2$, $w_4 = k_3 N_2 N_1$, $w_5 = d_3 N_3$, and $w_6 = k_4 N_3 N_1$. To obtain the kinetics on the biologically reasonable time scale, the corresponding rate constants were set as $k_2 = k_3 = 10^{-5}$ s^{-1}, $k_4 = 10^{-6}$ s^{-1}, and $d_2 = d_3 = 1$ s^{-1}. In addition, r_a was chosen as a governing parameter and varied in the range from 1 to 10 s^{-1}.

The MC and MF kinetics calculated with the specification above are in good agreement (Fig. 1) despite the stochastic behavior of N_3. The MC and MF dependences of $\langle t_{\rm FP} \rangle$ on r_a are in good agreement as well (Fig. 2). For the standard deviation of $t_{\rm FP}$, as expected, the agreement between the MC
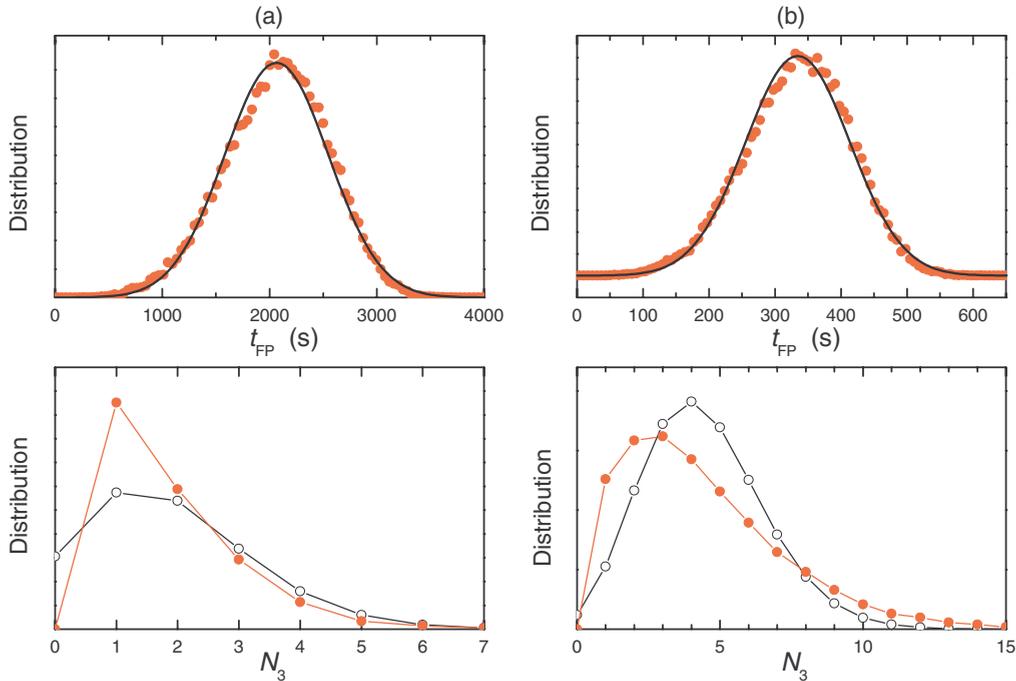
FIG. 4. (Color online) Distributions of $t_{\rm FP}$ and N_3 for $r_a = 1$ (a) and 10 s^{-1} (b). The MC distribution of $t_{\rm FP}$ (circles) is shown together with the Gaussian distribution (lines) $f(x) = (2\pi \langle \Delta x \rangle^2)^{-1/2} \exp[-(\Delta x)^2 / 2 \langle \Delta x \rangle^2]$, calculated by using the same average and variance as in the MC case. The MC distribution of N_3 (solid circles) is exhibited together with the Poissonian distribution (open circles) $f(N) = \langle N \rangle \exp(-\langle N \rangle)/N!$, calculated by employing the same average as in the MC case.

and MF results is somewhat worse (Fig. 2). Specifically, the MC deviation is larger by a factor of 1.1–2. The average value of N_3 is slightly larger in the MC case as well (Fig. 3). The distribution of t_{FP} is Gaussian (Fig. 4, top panels), while the distribution of N_3 exhibits, as expected (because the P_a association with C_3 is irreversible), deviations from the Poissonian one (Fig. 4, bottom panels). The deviations are, however, modest.

IV. APPLICATION

Our present study was initiated by the experiments performed in our group [11] with the aim to clarify the mechanism of the pore formation and membrane destabilization observed during interaction of highly active α-helical peptide with sub-100-nm lipid vesicles that mimic enveloped viruses with nanoscale membrane curvature. The distributions of the time of the first-pore formation, $F(t_{FP})$ [Figs. 5(a) and 5(b)] were obtained from single-vesicle imaging for vesicles with average radii of 100 and 40 nm. The distributions of vesicles over the radius $f(r)$ were relatively narrow [Fig. 5(c)]. With decreasing the average vesicle radius from 100 nm to 40 nm, $\langle t_{FP} \rangle$ is found to become appreciably shorter, i.e., t_{FP} depends on r and becomes shorter with decreasing r. The ratio $\langle (\Delta t_{FP})^2 \rangle^{1/2} / \langle t_{FP} \rangle$ is slightly larger for smaller vesicles. In addition, the distribution of t_{FP} for smaller vesicles exhibits a tail, while the distribution for larger vesicles is nearly symmetric.

Due to the dependence of t_{FP} on r, the experimentally observed distributions $F(t_{FP})$ depend not only on the kinetics of pore formation (as discussed in Secs. II and III), but also on $f(r)$. If the latter dependence dominate, $F(t_{FP})$ can be expressed via $f(r)$ as

$$F(t_{FP}) = f(r(t_{FP})) \frac{dr(t_{FP})}{dt_{FP}}, \qquad (24)$$

where $r(t_{FP})$ is the function inverse to $t_{FP}(r)$.

Physically, the dependence of t_{FP} on r may be related to two factors. The first one is that the pore-formation rate is proportional to the vesicle area. The second one is that the activation energy for this process may decrease with decreasing r due to curvature-related membrane strain (as discussed in the other context in Ref. [14]). With decreasing r, t_{FP} is expected to increase according to the former factor and decrease according to the latter factor. In the case under consideration, as already noted, the experiment indicates that t_{FP} decreases with decreasing r and accordingly the curvature-related membrane strain seems to dominate. Taking only this factor into account, we represent the dependence of t_{FP} on r as [14]

$$t_{FP}(r) = t_{\circ} \exp(-Ba/r), \qquad (25)$$

where $t_{\circ}$ is the value at $r \to \infty$, $a = 2.5$ nm is the thickness of the lipid layer, and B is a dimensionless parameter related to expansion of the activation energy with respect to the lipid-bilayer curvature.

To reproduce the position of peaks in the distributions of t_{FP} for vesicles with $\langle r \rangle = 100$ and 40 nm [Figs. 5(a) and 5(b)], we have used Eqs. (24) and (25) with $t_{\circ} = 15$ min, $B = 30$, and the experimentally measured vesicle size distributions [Fig. 5(c)].
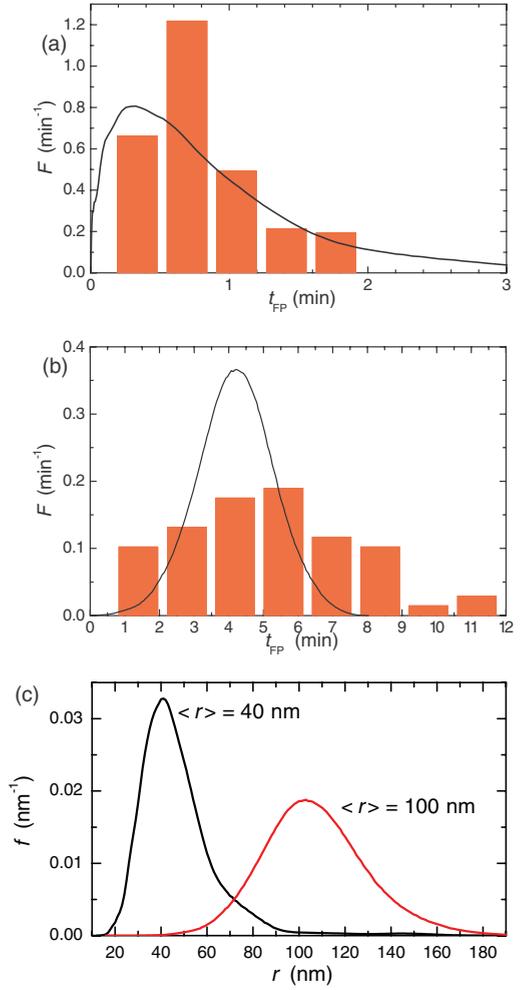

FIG. 5. (Color online) Distribution of the time of formation of the first pore by α-helical peptide in vesicles with an average radius of (a) 100 and (b) 40 nm. The columns show the experimental data (reproduced from Fig. 3 in Ref. [11]). The solid lines were obtained by taking the dependence of t_{FP} on the vesicle radius into account [Eqs. (24) and (25)]. (c) The distributions of vesicles over radius were obtained by the nanoparticle tracking analysis.

The distributions $F(t_{FP})$ calculated with these parameters are shown in Figs. 5(a) and 5(b). Comparing the experimental and theoretical results, one can notice that for smaller vesicles [with $\langle r \rangle = 40$ nm; see Fig. 5(a)] the calculated full width at half maximum (FWHM) of $F(t_{FP})$ is comparable to that observed experimentally (in both cases, the FWHM is approximately equal to 1.1 min). In addition, the model reproduces the experimentally observed asymmetry (tail) in the distribution of t_{FP}, which appears to be related to the corresponding asymmetry of the size distribution of smaller vesicles. For larger vesicles [Fig. 5(b)], the calculated FWHM ($\simeq 2.5$ min) is appreciably smaller than in the experiment ($\simeq 7$ min). The latter seems to indicate that for these vesicles the contribution of fluctuations of the number of attached peptides to FWHM is comparable to or slightly larger that that related to the vesicle size distribution. This conclusion is confirmed by our MC simulations (Fig. 4) showing that the fluctuation-related scale of the ratio $\langle (\Delta t_{FP})^2 \rangle^{1/2} / \langle t_{FP} \rangle$ may be comparable to that observed for larger vesicles [Fig. 5(b)].

V. CONCLUSION

Motivated by the experimental studies of interaction of lytic peptides with lipid vesicles, virions, or bacteria, we have analyzed in detail the generic model describing peptide attachment and peptide-induced and nucleation-limited pore formation. The dependences of the corresponding first-passage time t_{FP} and its standard deviation on the model parameters have been calculated analytically [expressions (11) and (13)] by using the MF equations and also by employing MC simulations. The MC simulations indicate that the MF predictions for t_{FP} are fairly accurate even in the situations when there are only a few precritical nuclei. The analytical predictions for the standard deviation of t_{FP} are less accurate. In particular, the standard deviation calculated analytically may be smaller compared to the MC one by a factor of 1.1–2.

Our analysis of the standard deviation of t_{FP} has been focused on the role of fluctuations of the number of peptides attached to a vesicle. The corresponding expression (13) can be used to describe pore formation in an ensemble of vesicles provided that they are of the same size. In real experiments, vesicles always have some variation in size. Taking into account that t_{FP} depends on the vesicle size, the standard deviation of t_{FP} should contain the related contribution. For a given dependence of t_{FP} on the vesicle size, the latter contribution to the standard deviation of t_{FP} can be calculated by employing Eq. (24) provided that the vesicle distribution is known.

The results obtained have been used to interpret the recent experiments [11] with highly active α-helical peptide and sub-100-nm vesicles. In particular, our analysis indicates that the contribution of fluctuations of the number of peptides, attached to a vesicle, to the ratio $\langle(\Delta t_{FP})^2\rangle^{1/2}/\langle t_{FP}\rangle$ can be comparable to that observed experimentally. Thus the fluctuations appear to be manifested in the kinetics despite the effects related to the vesicle-size distribution.

[1] S. M. Kathmann, Theor. Chem. Acc. **116**, 169 (2006).

[2] I. J. Ford, Proc. Inst. Mech. Eng. C **218**, 883 (2004); S. M. Kathmann, G. K. Schenter, B. C. Garrett, B. Chen, and J. I. Siepmann, J. Phys. Chem. C **113**, 10354 (2009).

[3] I. J. Ford, Phys. Rev. E **56**, 5615 (1997).

[4] L. Maibaum, Phys. Rev. Lett. **101**, 256102 (2008); M. Horsch, J. Vrabec, and H. Hasse, Phys. Rev. E **78**, 011603 (2008); S. V. Vosel, A. A. Onischuk, and P. A. Purtov, J. Chem. Phys. **131**, 204508 (2009); I. Napari, J. Julin, and H. Vehkamaki, *ibid.* **131**, 244511 (2009); L. Filion, M. Hermes, R. Ni, and M. Dijkstra, *ibid.* **133**, 244115 (2010); S. Ryu and W. Cai, Phys. Rev. E **82**, 011603 (2010); K. K. Tanaka, H. Tanaka, T. Yamamoto, and K. Kawamura, J. Chem. Phys. **134**, 204313 (2011); Y. Liu, Y. Men, and X. Zhang, *ibid.* **135**, 184701 (2011).

[5] A. M. Morris, M. A. Watzky, and R. G. Finke, Biochim. Biophys. Acta **1794**, 375 (2009).

[6] E. C. Neyts and A. Bogaerts, J. Phys. Chem. C **113**, 2771 (2009); M. Schwind, V. P. Zhdanov, I. Zorić, and B. Kasemo, Nano Lett. **10**, 931 (2010); V. P. Zhdanov, M. Schwind, I. Zorić, and B. Kasemo, Physica E **42**, 1990 (2010); Y. Shibuta and T. Suzuki, Chem. Phys. Lett. **498**, 323 (2010); P. Palanisamy and J. M. Howe, J. Appl. Phys. **110**, 024908 (2011).

[7] D. De Sancho and R. B. Best, J. Am. Chem. Soc. **133**, 6809 (2011); O. V. Galzitskay and A. V. Glyakina, Proteins: Struct. Funct. Bioinf. **80**, 2711 (2012); L. H. Greene and T. M. Grant, FEBS Lett. **586**, 962 (2012); B. G. Wensley, L. G. Kwa, S. L. Shammas, J. M. Rogers, and J. Clarke, J. Mol. Biol. **423**, 273 (2012).

[8] P. Brocos, P. Mendoza-Espinosa, R. Castillo, J. Mas-Oliva, and A. Pineiro, Soft Matter **8**, 9005 (2012); S. Gudlur, P. Sukthankar, J. Gao, L. A. Avila, Y. Hiromasa, J. Chen, T. Iwamoto, and J. M. Tomich, PLoS ONE **7**, e45374 (2012); S. Rudorf and J. O. Rädler, J. Am. Chem. Soc. **134**, 11652 (2012).

[9] K. A. Brogden, Nat. Rev. Microbiol. **3**, 239 (2005); H. Sato and J. B. Feix, Biochim. Biophys. Acta **1758**, 1245 (2006); G. Fuertes, D. Gimenez, S. Esteban-Martin, O. L. Sanchez-Munoz, and J. Salgado, Eur. Biophys. J. **40**, 399 (2011); V. Teixeira, M. J. Feio, and M. Bastos, Prog. Lipid Res. **51**, 149 (2012).

[10] J. E. Cummings and T. K. Vanderlick, Biochemistry **46**, 11882 (2007); G. van den Bogaart, J. V. Guzman, J. T. Mika, and B. Poolman, J. Biol. Chem. **283**, 33854 (2008); M. D. Bobardt, G. Cheng, L. de Witte, S. Selvarajah, U. Chatterji, B. E. Sanders-Beer, T. B. H. Geijtenbeek, F. V. Chisari, and P. A. Gallay, Proc. Natl. Acad. Sci. USA **105**, 5525 (2008); S. M. Gregory, A. Cavenaugh, V. Journigan, A. Pokorny, and P. F. F. Almeida, Biophys. J. **94**, 1667 (2008); P. F. Almeida and A. Pokorny, Biochemistry **48**, 8083 (2009); M. Gregory, A. Pokorny, and P. F. F. Almeida, Biophys. J. **96**, 116 (2009); N.-J. Cho, H. Dvory-Sobol, A. Xiong, S.-J. Cho, C. W. Frank, and J. S. Glenn, ACS Chem. Biol. **4**, 1061 (2009); B. Apellaniz, J. L. Nieva, P. Schwille, and A. J. Garcya-Saez, Biophys. J. **99**, 3619 (2010); C. Mazzuca, B. Orioni, M. Coletta, F. Formaggio, C. Toniolo, G. Maulucci, M. De Spirito, B. Pispisa, M. Venanzi, and L. Stella, *ibid.* **99**, 1791 (2010); P. Wadhwani, J. Reichert, J. Burck, and A. S. Ulrich, Eur. Biophys. J. **41**, 177 (2012).

[11] S. R. Tabaei, M. Rabe, V. P. Zhdanov, N.-J. Cho, and F. Höök, Nano Lett. **12**, 5719 (2012).

[12] L. Gao and W. Fang, Soft Matter **5**, 3312 (2009); R. Chen and A. E. Mark, Eur. Biophys. J. **40**, 545 (2011); A. D. Cirac, G. Moiset, J. T. Mika, A. Kocer, P. Salvador, B. Poolman, S. J. Marrink, and D. Sengupta, Biophys. J. **100**, 2422 (2011); H.-J. Woo and A. Wallqvist, J. Phys. Chem. B **115**, 8122 (2011).

[13] K. Matsuzaki, O. Murase, and K. Miyajima, Biochemistry **34**, 12553 (1995); L. Becucci and R. Guidelli, Langmuir **23**, 5601 (2007); H. W. Huang, Biophys. J. **96**, 3263 (2009).

[14] V. P. Zhdanov and F. Höök, Biophys. Chem. **170**, 7 (2012).